

# DesignCon 2007

## Crosstalk due to Periodic Plane Cutouts

Jason R. Miller, Sun Microsystems

Gustavo Blando, Sun Microsystems

Istvan Novak, Sun Microsystems

## Abstract

As board designs get denser signal traces are often forced to route in proximity to board plane cutouts. Along the length of the trace, the trace may periodically encounter a cutout due to connector pin fields, via transitions, etc. In this paper, the impact of periodic, layer-to-layer coupling on far-end and near-end crosstalk is examined. The coupling is found to increase the near-end and far-end coupling and introduce periodic peaks in the near-end coupling profile. Realistic thermal relief patterns and antipads extracted from board designs are simulated. Frequency domain measurement results are correlated to simulation.

## Author(s) Biography

Jason Miller is currently a senior staff engineer at Sun Microsystems where he works on ASIC development, ASIC packaging, interconnect modeling and characterization, and system simulation. He received his Ph.D. in Electrical Engineering from Columbia University.

Gustavo Blando is a signal integrity engineer with over 10 years of experience in the industry. Currently at Sun Microsystems he is responsible for the development of new processes and methodologies in the areas of broadband measurement, high speed modeling and system simulations. He received his M.S. from Northeastern University.

Istvan Novak is a signal-integrity senior staff engineer at Sun Microsystems, Inc. Besides signal integrity design of high-speed serial and parallel buses, he is engaged in the design and characterization of power-distribution networks and packages for Sun servers. He creates simulation models, and develops measurement techniques for power distribution. Istvan has twenty plus years of experience with high-speed digital, RF and analog circuits, and system design. He is a Fellow of IEEE for his contributions to the fields of signal-integrity, RF measurements, and simulation methodologies.

## Introduction

In dense multilayer boards, traces may have to be routed through regions containing packages, connectors, and/or multi-pin sockets. In these regions the trace may periodically encounter regular patterns of via barrels, antipad cutouts, BGA solderballs, etc. In an earlier work, we showed that although the reflection at each discontinuity is small, the periodicity of the structure lines up these reflections and if this loading carries on for an extended length, the slope of the loss curve ( $S_{12}$ ) will be increased by the presence of resonance dips in the loss profile [1]. For typical geometries, this loss was found to be modest when the trace maintained a distance from the cutout. However, the additional attenuation starts to sharply increase as the separation between the antipad and trace approaches zero. Other significant findings of this study were that the separation between the periodic discontinuities determined the minimum frequency of these dips ( $\lambda/2$ ) and that the magnitude of the dip scales with the number of discontinuities. In this paper, we extend this earlier work to examine the impact of periodic cutouts on layer-to-layer crosstalk.

Crosstalk is caused by the coupling of energy from one trace to another. Figure 1 shows two coupled transmission lines which are used here to define the relevant terms and quantities. The crosstalk observed on the victim line at port 2 is called the near-end crosstalk (NEXT). NEXT is proportional to the sum of the capacitive and inductive couplings and as such it appears on both microstrips and stripline traces. The crosstalk at port 4 is called the far-end crosstalk (FEXT) and is proportional to the difference in the capacitive and inductive coupling. Consequently, FEXT is zero for homogenous structures such as a stripline. Note that the port numbering scheme shown in Figure 1 is followed throughout this paper. Light coupling between the traces and matched terminations on all four ports is assumed. The assumption of light coupling guarantees a small difference between the modal impedances, hence a single resistive termination is enough to keep the mode conversion low.

To establish the baseline, first we simulate a coupled microstrip trace pair over solid ground, where the traces are on the same side of the plane. Figure 2 shows the simulated frequency domain response at port 2, port 3 and port 4 ( $S_{12}$ ,  $S_{13}$ , and  $S_{14}$ , respectively) for a pair of 10-inch, edge-coupled microstrip traces spaced 3 mils apart. At low frequencies, both  $S_{12}$  and  $S_{13}$  have rising slopes. The first maxima of the  $S_{12}$  profile occurs at  $\lambda/4$  of the coupled line length. The subsequent peaks occur at the odd harmonics of  $\lambda/4$ . The  $S_{14}$  profile reaches full coupling at frequencies where the time-of-flight difference of the even and odd modes equals half of the period. The subsequent  $S_{14}$  peaks occur at odd harmonics of the fundamental. The  $S_{13}$  profile has corresponding minima at the frequencies where the far-end coupling peaks. This can be explained by conservation of energy. Note that the finite losses create an overall negative slope on all of the traces. The baseline example shown in Figure 2 is for a microstrip, since it exhibits both finite NEXT and FEXT. For a homogenous stripline, the baseline results show similar characteristics for NEXT, but FEXT is zero.

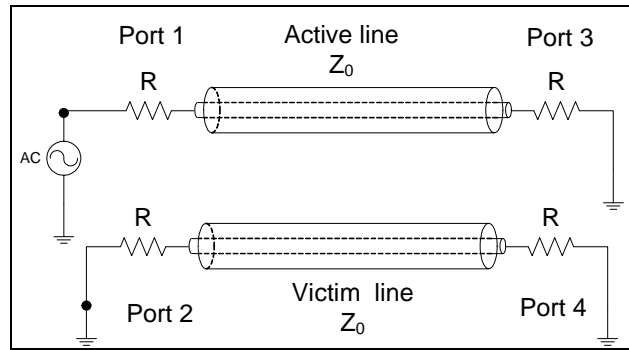


Figure 1: Two coupled transmission lines. The traces are assumed to be terminated in  $Z_0$ .

If two traces exist on opposite sides of a solid plane, either stripline or microstrip, the crosstalk at high frequencies approaches zero, because the return currents are confined to thin layers on the top and bottom surfaces of the planes, effectively separating the two current loops. However, when the plane separating the traces above and below has cutouts near the traces, the openings behave like small apertures, through which the field can spill over from one side to the other. Such cutouts can come from antipad cutouts in the PCB stackup.

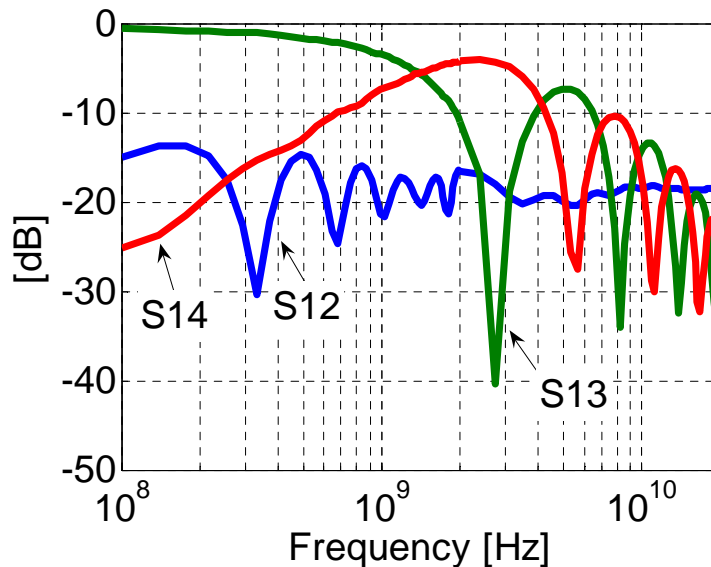


Figure 2: Frequency response of a coupled microstrip simulated at three port locations.

Traces can get routed near to or over antipad cutouts and thermal reliefs due to misregistration and manufacturing tolerances. Figure 3 illustrates a trace of width,  $w$ , routed through a pair of antipads. The trace keeps a distance,  $s$ , from one of the antipad cutouts. For example, take the case of a 4-mil ( $w = 4$  mils), board trace routed through a package pin field with a 1 mm pitch BGAs. A typical antipad diameter is 30 mils. Typical tolerances for same core misregistration is

+/-3 mils. In this example, the tolerances can place the trace 1.315 mils *over* the antipad edge (i.e.  $s = -1.315$  mils). If the antipad cutout and trace are on different cores, the antipad to trace overlap can be even greater; typical tolerances for different core misregistration are +/-5 mils. This can put the trace 3.315 mils *over* the antipad edge (i.e.  $s = -3.315$  mils).

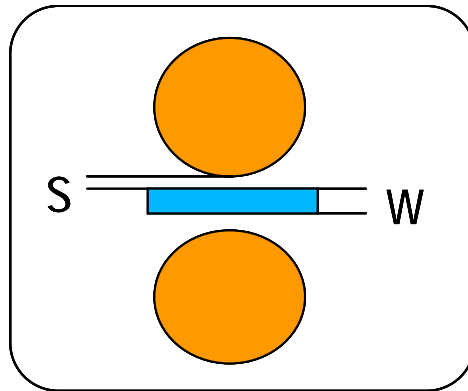


Figure 3: Illustration of trace routed through a pin field which could represent a BGA or connector, for example.

This paper will examine the impact of such periodic cutouts on layer to layer crosstalk. In the first section, we show the results from measurements of test structures which route traces at different distances from periodic cutouts. The second section seeks to validate these measurements through correlation with full-wave field-solver simulations. Finally, in the third section, we examine how the periodic coupling scales with the spacing between the trace and the cutout and how the periodic coupling scales with the number of cutouts.

## 1. Test board measurements

Test boards were designed and fabricated to evaluate the impact of the periodic cutouts on layer-to-layer crosstalk. The test board consisted of a pair of 1-inch long, serpentine traces routing through a pin field at three different distances from the cutout. Table 1 lists the relevant portion of the board stackup. The serpentine traces on layer 14 and layer 16 are identically routed on either side of perforated plane on layer 15. The antipad holes in layer 15 extend through all three plane layers (layers 12 through 17). Layer 14 (signal 4) is depopulated. Vias stitch the planes together and where the vias connect to the plane, a thermal relief pattern is used (see Figure 4). Figure 4 shows a snapshot of the serpentine route on top of layer 15. Trace 1, shown on the top of Figure 4, is centered between the antipad field, trace 2 runs alongside the perimeter of the antipad cutout but not over the cutout, and trace 3 passes over the cutouts.

The four columns of antipad holes shown in Figure 4 represent a “unit cell” (for instance a connector pin field), which is repeated six times along the length of the trace. The total conductor length is 2879 mils. The separation between antipad cutouts within a unit cell horizontally is 75 mils. The length of the conductor for each unit cell is 474 mils.

Layer Number	signal / plane	Copper Thickness (mil)	Dielectric Thickness (mil)
12	PWR4	1.2	
			4.00
13	S4	0.6	
			3.88
14	S5	0.6	
			4.00
15	GND5	1.2	
			3.94
16	S6	0.6	
			5.90
17	GND6	0.6	

Table 1: Stackup of the test board.

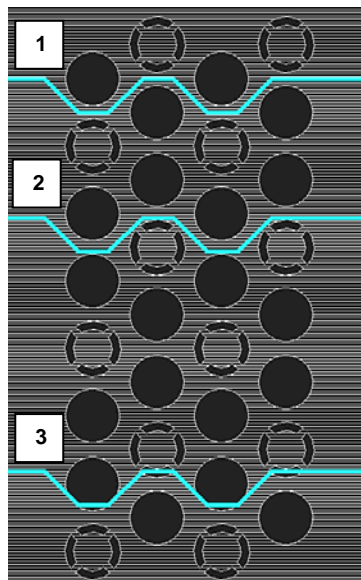


Figure 4: Snapshot of the test board. FR4 dielectric material was used.

Measurements were performed using differential 500 $\mu$ m GSSG (Ground-Signal-Signal-Ground) picoprobes. A SOLT calibration was performed on all four ports using the picoprobes and a calibration standard substrate. The board was machine milled down to two different depths in order to contact the two traces on the two different layers. Special horseshoe-shaped pads were used in the board design to provide ground lands for the probe on all signal layers. After milling, the picoprobes were placed into position directly on the traces and ground pads at either end of the structure. Four-port S-parameters were captured with an Agilent N4230A VNA from 300kHz to 20GHz using a linear sweep with 1601 points and an IF bandwidth of 300Hz. Figure 5 shows a photograph of the picoprobe landed on the trace and ground pads.

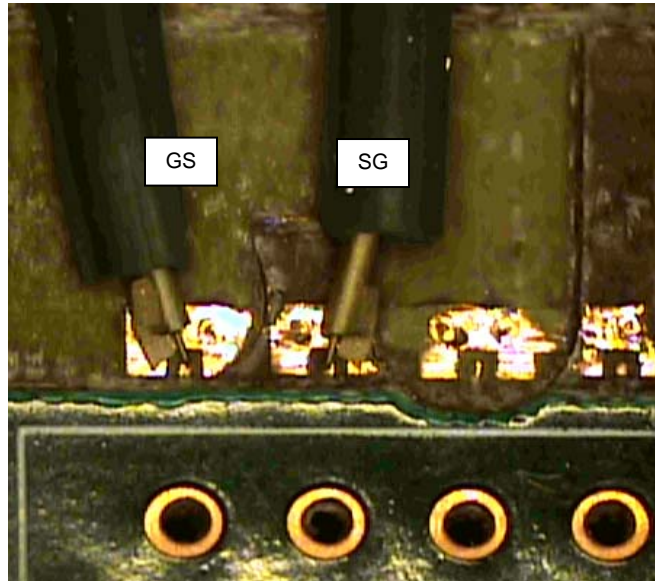


Figure 5: Photo of the test structure with probes landed on two traces of a differential pair. The horseshoe shaped ground pads are visible. Near these horse-shoe connections the spacing between the traces is increased to facilitate easier connections to wafer probes. The traces are running vertically, from the probe tips downwards. The four large through holes form the first set of vias creating the perforation.

Figure 6-8 show the measured S12 profile, S14 profile, and the S13 profile for the three test cases, respectively. The S12 and S14 profiles show that as the trace passes closer to the antipad holes the trace-to-trace coupling significantly increases. Note that with a solid plane with no antipads, both S12 and S14 would be nominally zero. The extra loss observed in the S13 profile is due to the periodical discontinuities introduced by the antipads and vias, and described in detail in [1].

Figure 9 permits a closer inspection of the S12 profile for trace 3. The first maxima of the S12 profile occurs at  $\lambda/4$  of the total line length, here 2879 mils. The subsequent peaks occur at the odd harmonics of  $\lambda/4$ , as expected. However, starting at about 5.77 GHz, there is the appearance of an additional series of higher magnitude peaks. These peaks are a consequence of the periodic discontinuities in the test structure. Specifically, the center frequency of the peaks corresponds to  $\lambda/2$  of the unit cell length, here 474 mils. The subsequent peaks are at harmonics of the fundamental. Traces 2 and 3 show the same center frequencies. Figure 10 plots the S12 for trace 3 and trace 2. Comparing the envelope of the  $\lambda/4$  series to the first peak of the  $\lambda/2$  series, the relative increase in S12 is 8.4 (40%) and 10 dB (21%) for trace 3 and trace 2, respectively.

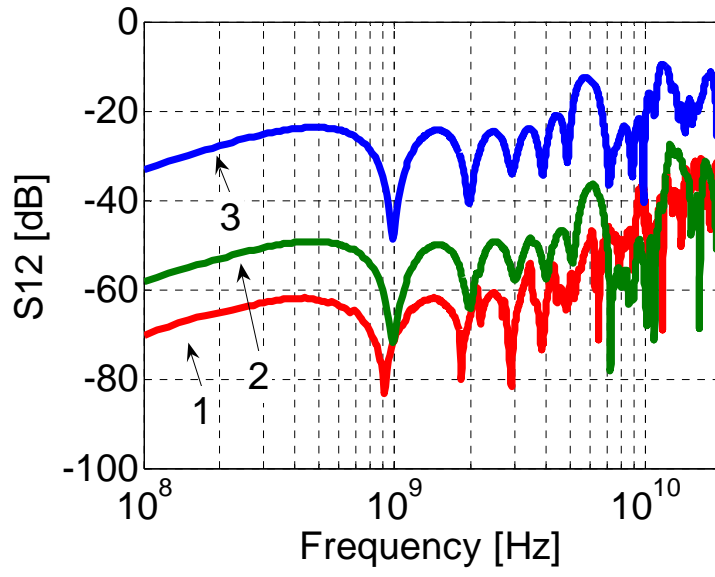


Figure 6: Measured S12 for the three test cases.

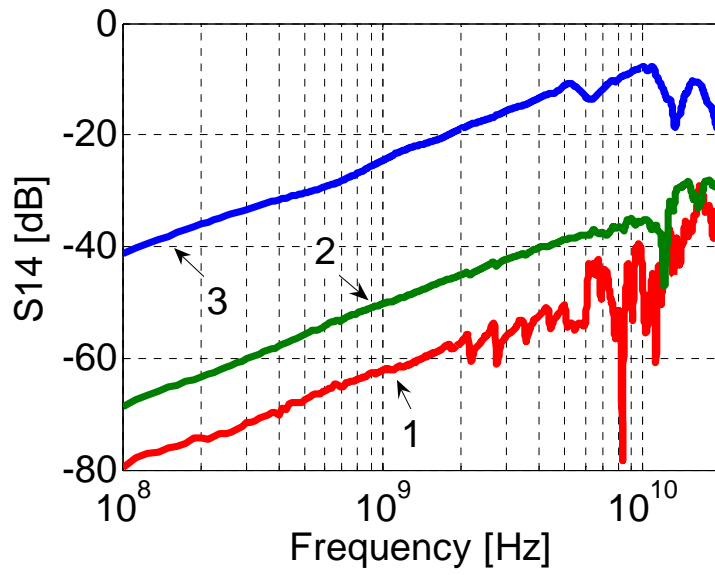


Figure 7: Measured S14 for the three test cases.



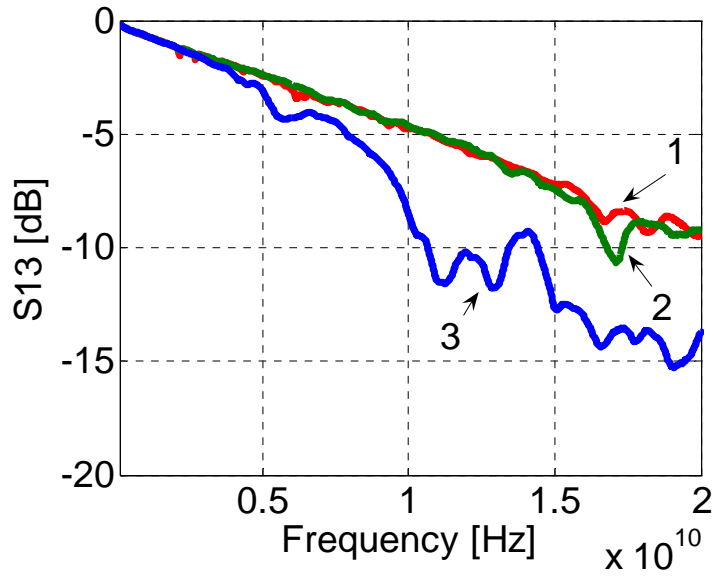


Figure 8: Measured S13 (insertion loss) for the three test cases.

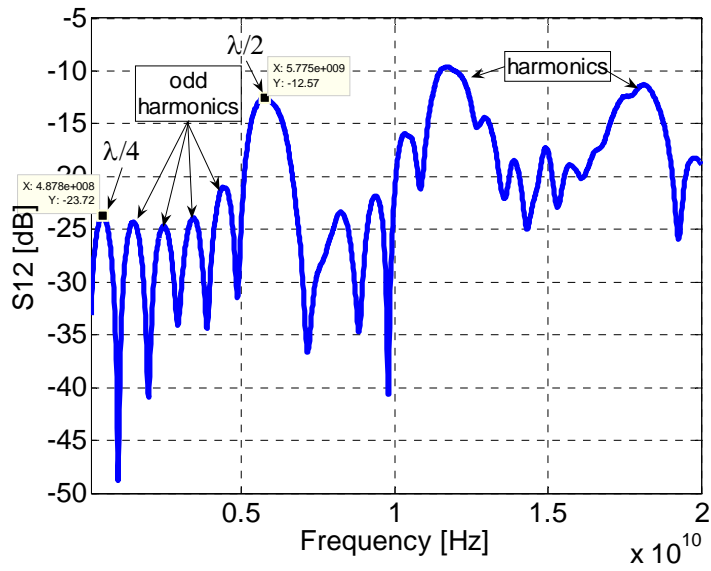


Figure 9. Measured S12 for trace 3.

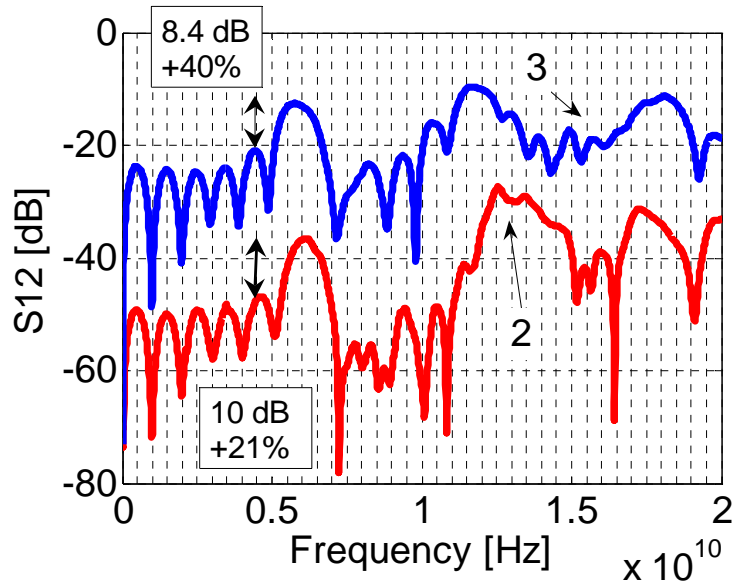


Figure 10: Plot of S12 showing the relative increase in near end coupling due to the periodic cutouts in the vicinity of trace 3 and trace 2.

## 2. Measurement to simulation correlation

HFSS [2], a full-wave 3-D field solver, was used to solve for the S-parameters of the test structure. Because the physical size of the test structure was large compared to the wavelengths involved, the complete structure with all of its details quickly overwhelmed the compute resources. To simplify the structure, the thermal relief pattern was not included in the simulation – only the plane cutouts were used with a diameter matching the outer diameter of the thermal-relief pattern. Consequently, the location of the vias, which stitch the planes together, was placed outside of the pin field, on the edge of the geometry. Another simplification was that only the antipad holes nearest to the trace were included; the plane was solid beyond the vicinity of the trace. Figure 11 shows a snapshot of the simulated geometry. A wideband causal model was used to capture the frequency dependence of the dielectric material [3]. These geometrical simplifications limited our range of simulation accuracy to approximately 10 GHz.

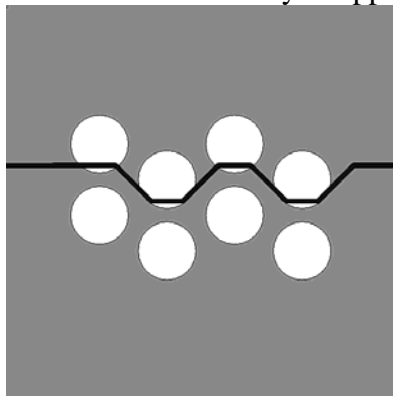


Figure 11: Simulation model of the simplified unit cell, showing trace 3.

Figures 12 and Figure 13 plot the simulated S12 and S14 profiles, respectively, for trace 2 against measurement results. The correlation is good, capturing the center location and magnitude of all of the major peaks. Figures 14 and Figure 15 plot the simulated S12 and S14 profiles, respectively, for trace 3 against measurement results. Although the locations of the peaks are captured quite accurately by simulation there is some magnitude offset. The simulation overestimates the near-end and far-end coupling. This is consistent with the fact that the thermal reliefs were omitted in the simulation model, increasing the area of the plane cutouts and layer-to-layer coupling.

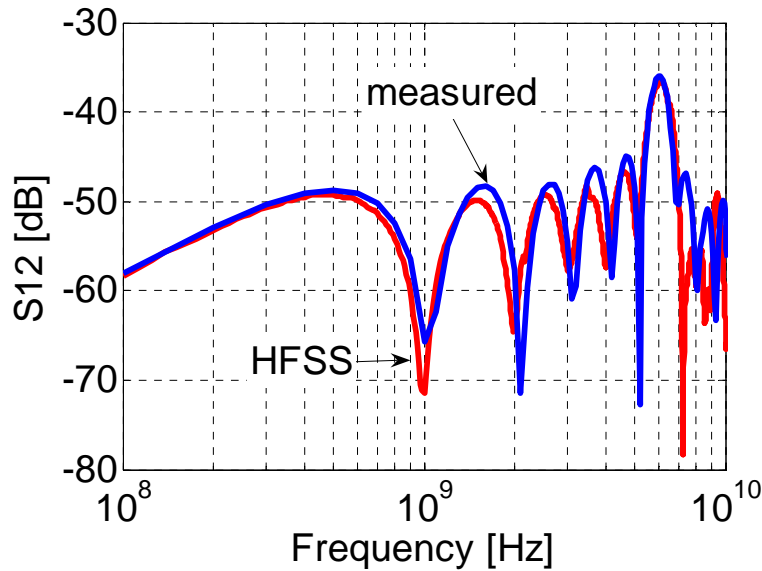


Figure 12: Measurement and simulation data plotted for S12 for trace 2.

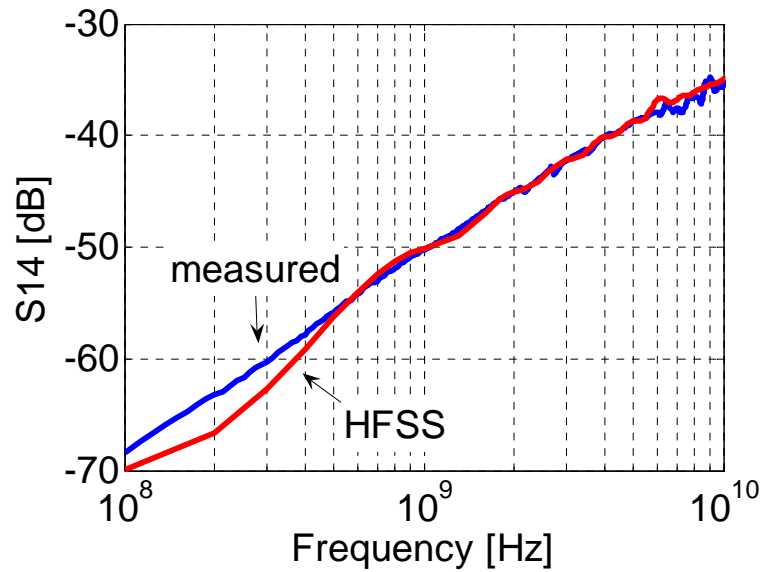


Figure 13: Measurement and simulation data plotted for S14 for trace 2.

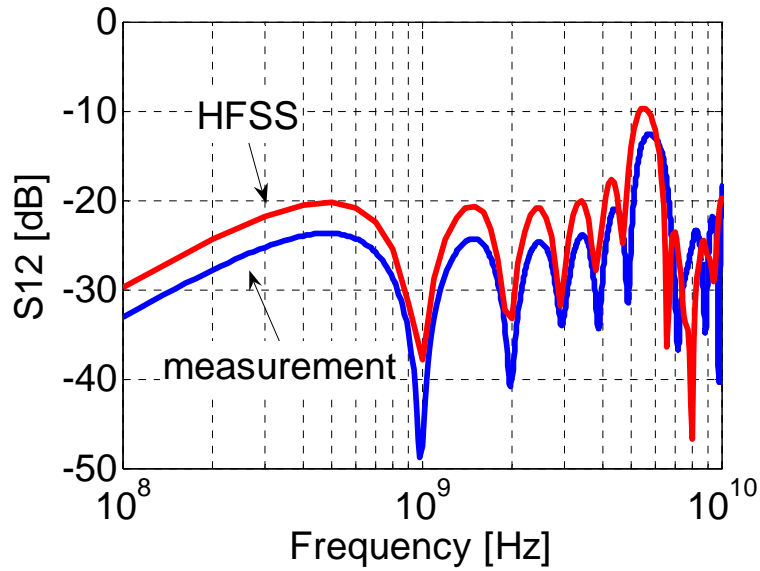


Figure 14: Measurement and simulation data plotted for S12 for trace 3.

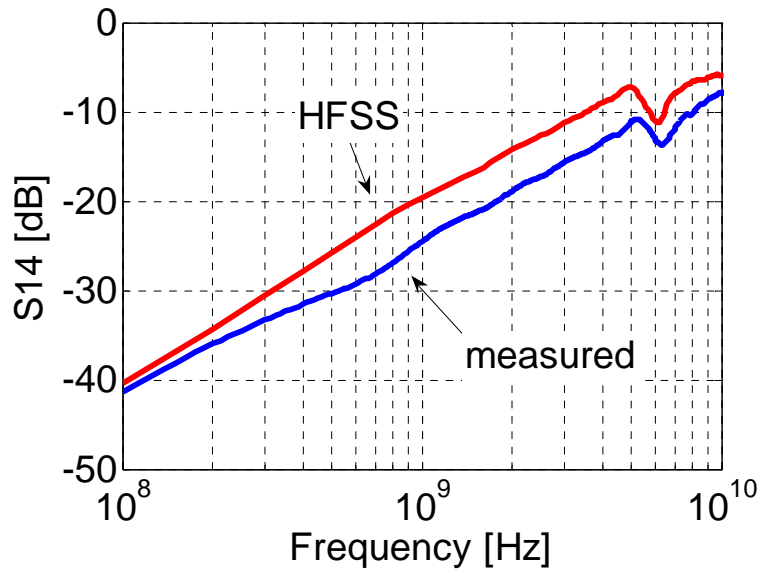


Figure 15: Measurement and simulation data plotted for S14 for trace 3.

### 3. Parameterization

With good correlation established between measurement and simulation, additional simulations were performed to examine how the periodic coupling scaled as several geometrical parameters were varied. Specifically, we examined how

- a. periodic coupling scales with the spacing between the trace and cutout
- b. periodic coupling scales with the number of cutouts

### 3.1 Parametrizing the spacing between trace and cutout

A 50-ohm stripline structure was created using 4-mil wide traces and 4+4-mil thick dielectrics, typical of PCB signal routes. The dielectric regions had a loss tangent of 0.02 and a relative dielectric constant of 4.5. A single cutout with a thermal relief pattern was located next to the trace and was centered along the length of the trace (see Figure 16). Simulation speed and accuracy was increased by simulating a single cutout (i.e. one unit cell) and then concatenating the unit cells in MATLAB using ABCD parameters. Using this approach, it was feasible to solve to a high-level of accuracy ( $\Delta S = 0.02$ ) in a relatively short amount of time. HFSS was used to simulate the structure.

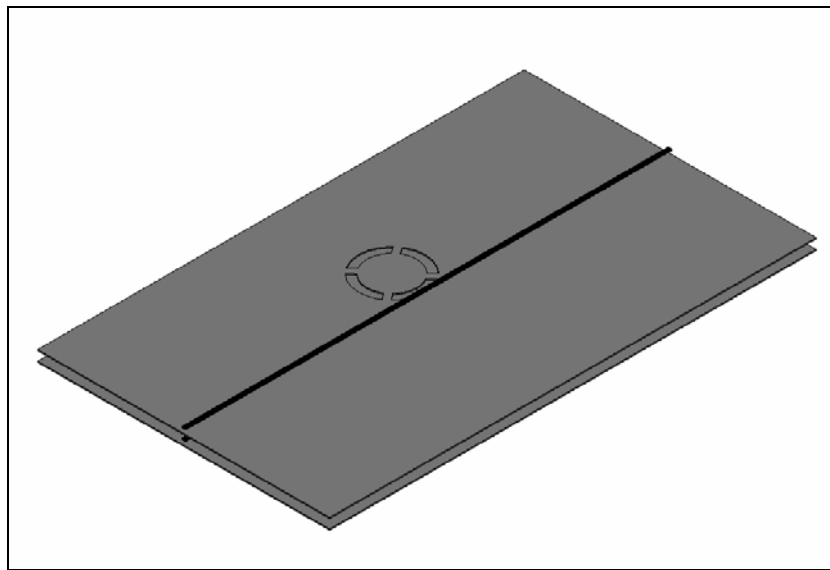


Figure 16. Simulated unit-cell structure used for parameterized sweeps.

For test case (a), the spacing between the trace and the perimeter of the cutout,  $s$ , was swept from  $s = 6$  mils to  $s = -8$  mils.  $s = 0$  means the trace routes along the edge of the cutout whereas a negative spacing means that the trace passed over the cutout. The unit-cell length was 500 mils; 20 unit cells were concatenated for a total length of 10 inches. Figure 17 and 18 plot  $S_{12}$  and  $S_{14}$ , respectively, for test case (a). As was observed in the measurement data, the first maxima of the  $S_{12}$  profile occurs at  $\lambda/4$  of the total line length, here 10 inches. The subsequent peaks occur at the odd harmonics of  $\lambda/4$ . Starting at about 5.45 GHz there is the appearance of an additional series of higher magnitude peaks. These peaks are a consequence of the periodic discontinuities in the test structure. Specifically, the peak corresponds to the frequency  $\lambda/2$  frequency of the unit cell length, here 500 mils. The subsequent peaks are at harmonics of the fundamental. The  $S_{14}$  profile also shows a series of peaks and dips starting at the  $\lambda/2$  frequency (5.45 GHz).

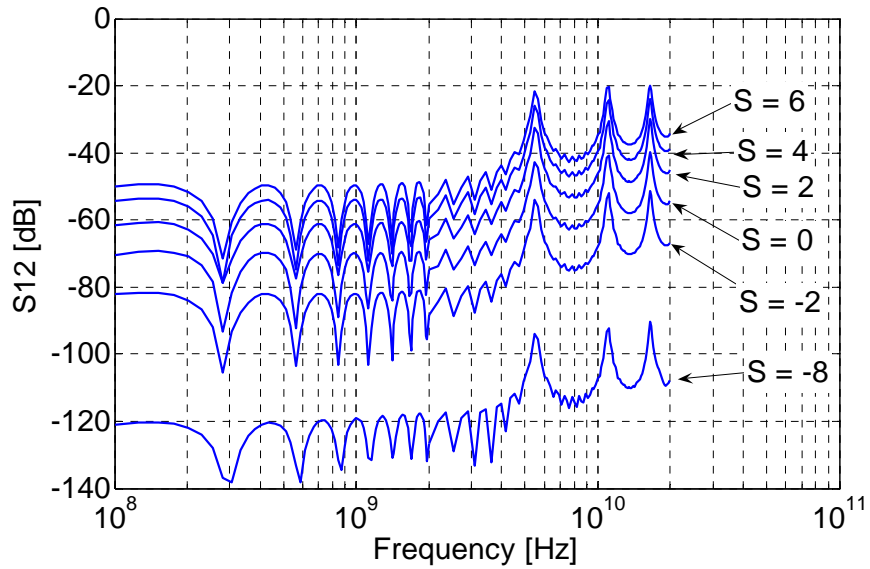


Figure 17: Plot of the S12 response for different spacings between the trace edge and cutout perimeter,  $s$ .

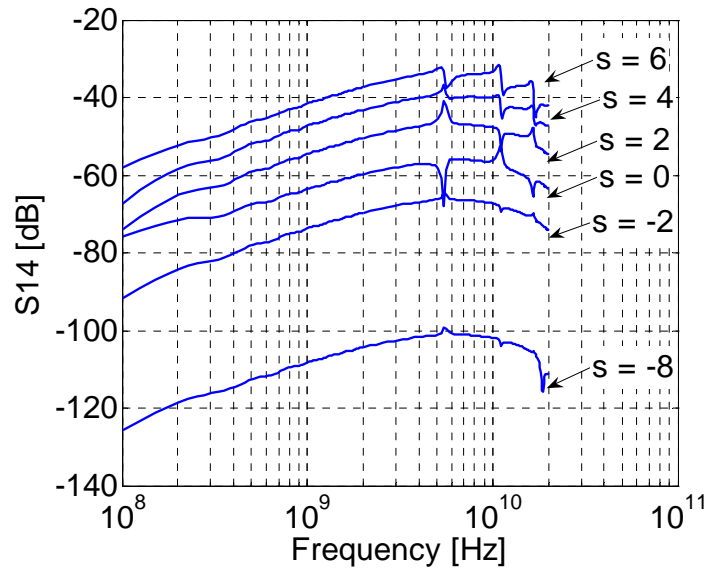


Figure 18: Plot of the S14 response for different spacings between the trace edge and cutout perimeter,  $s$ .

Figure 19 plots the S12 magnitude of the first  $\lambda/2$  peak at 5.45 GHz as a function of the spacing,  $s$ . S12 coupling increases at approximately 5-6 dB/mil as the trace moves closer to the cutout edge. With the trace 4 mils over the cutout, the coupling starts to saturate. Figure 20 plots the peak envelope of the S12 profile for the frequency range covering the  $\lambda/4$  fundamental and harmonics as a function of the spacing,  $s$ . Figure 21 plots the magnitude difference between the

$\lambda/4$  peak envelope and first  $\lambda/2$  peak. More than a 20 dB increase in the S12 coupling is observed across a wide range of trace edge to cutout edge separations.

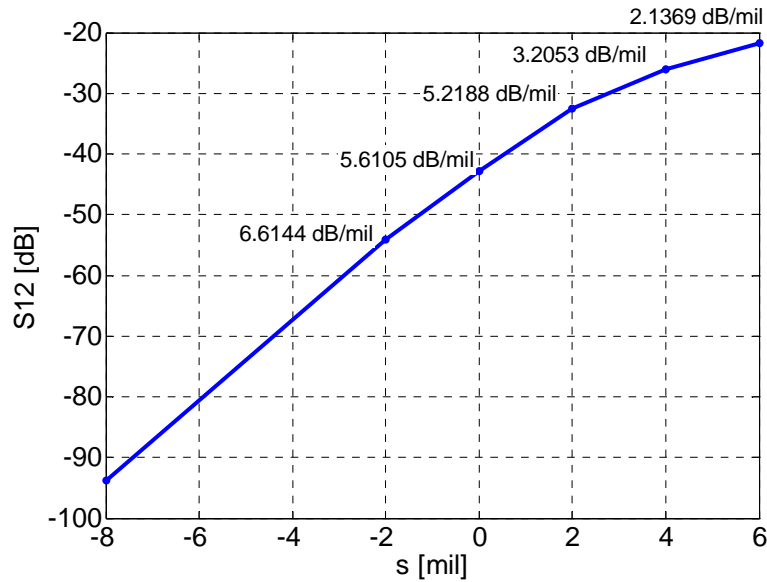


Figure 19: Plot of the S12 magnitude at the first  $\lambda/2$  peak as a function of the spacing between the trace edge and cutout perimeter, s.

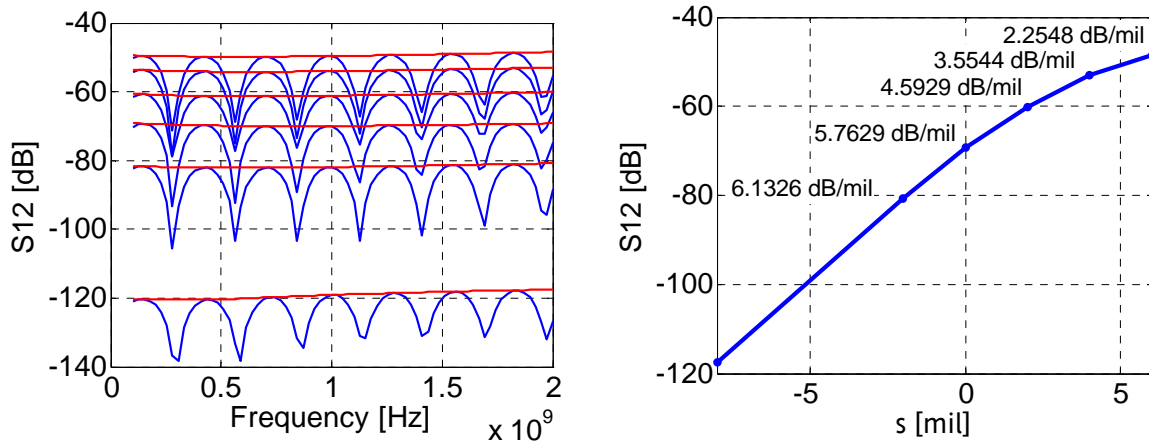


Figure 20: (a) Plot of the peak envelope of S12 as a function of the spacing between the trace edge and cutout perimeter, s. (b) Plot of the peak envelope (at 2 GHz) as a function of s. On the left plot, traces follow the same order, and have the same labels as traces in Figure 17.

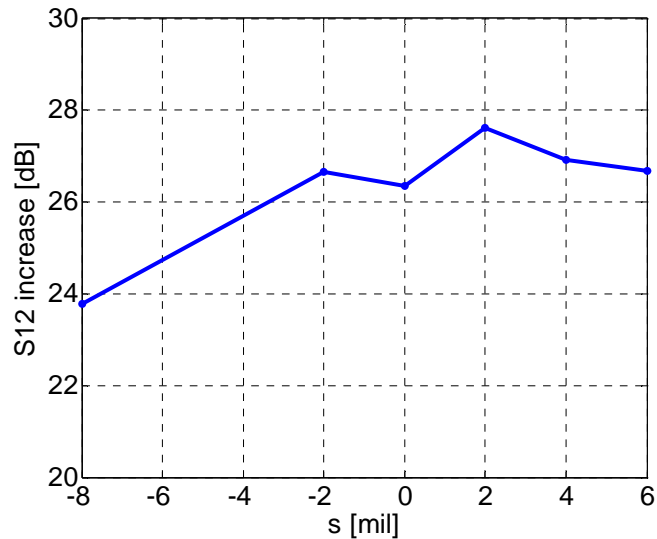


Figure 21: Plot of the magnitude difference between the first  $\lambda/2$  peak and the of the  $\lambda/4$  peak envelope.

### 3.2 Parametrizing the number of cutouts

For test case (b), the spacing between trace and cutout was set to zero ( $s = 0$ ) and the 500-mil unit cell was concatenated using the following number of unit cells: 5, 10, 20 and 30. Figure 22 plots S12 for test case (b) using 5 and 20 concatenated unit cells. With 5 unit cells, the  $\lambda/4$  fundamental is pushed to a center frequency four-times higher, corresponding to a factor-of-four decrease in the number of unit cells. The  $\lambda/2$  resonance, however, remains at the same frequency because the unit-cell length, which remained the same, dictates the location of the first  $\lambda/2$  peak. Figure 23 plots the magnitude of the first  $\lambda/2$  peak as a function of number of cells. As the number of cells increases the additional coupling introduced by each cell saturates. The curve saturates because eventually we get a uniform structure and the per-unit-cell characteristics become stable. Figure 22 shows that the  $\lambda/4$  series has a constant peak envelope, and is determined entirely by the unit-cell geometry. This coupling behaves like  $C_m$  and  $L_m$  in distributed coupled lines. Like in distributed coupled lines, these  $\lambda/4$  peaks do not depend on the actual length but only on the  $L_m/L$  and  $C_m/C$  per-unit-length ratios.



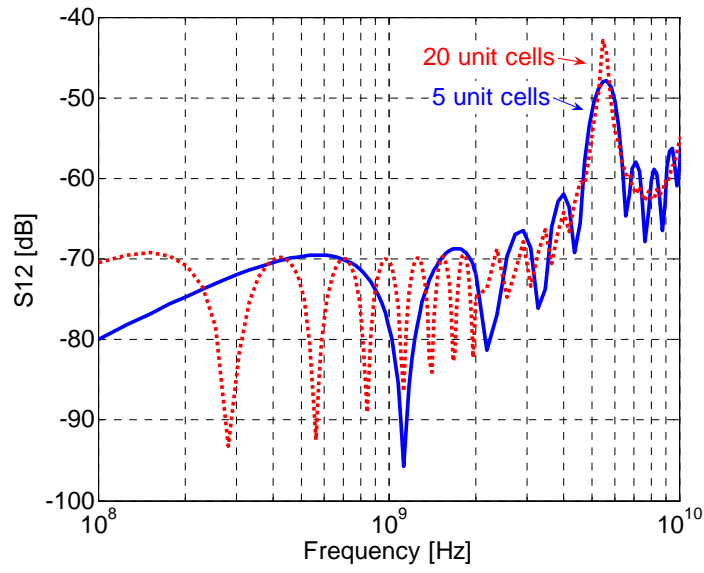


Figure 22: Plot of  $S_{12}$  for test case (b) using 5 and 20 concatenated unit cells.

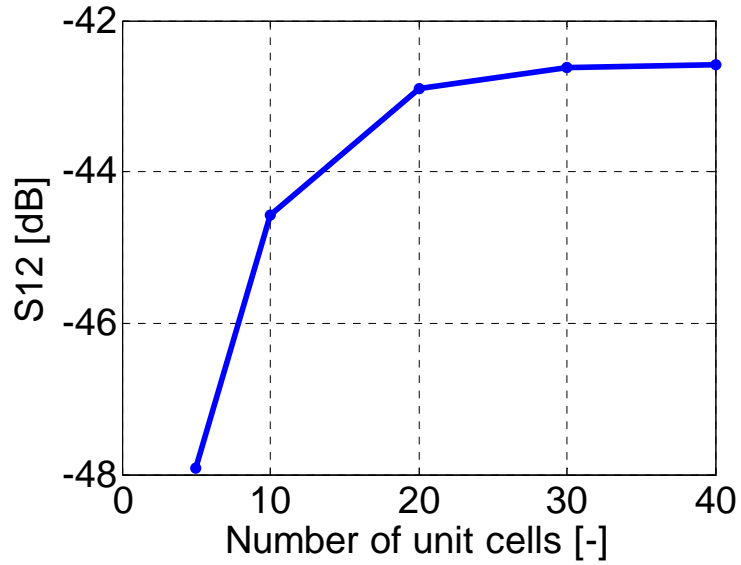


Figure 23: Plot of the  $S_{12}$  magnitude at the first  $\lambda/2$  peak as a function of the number of concatenated unit cells with a fixed spacing between the trace edge and cutout perimeter.

## Conclusions

Measured and simulated data of traces on opposite sides on a reference plane, passing close to or over periodic plane cutouts exhibit non-zero high-frequency crosstalk.

The near-end crosstalk due to periodic apertures show two distinct signatures: one component of the crosstalk looks very similar to the near-end crosstalk between uniform traces with distributed coupling, where the quarter-wave peaks are determined by the length of the full coupled length. With the geometries studied here, this part of the near-end crosstalk was below 1% even if the trace was accidentally routed over the voids. A second signature of near-end crosstalk showed up as harmonically related larger peaks, where the fundamental frequency corresponds to half of the wavelength between two adjacent cutouts. These peaks reach 1% coupling when the trace edge is aligned with the antipad edge, and reaches 10% when the trace is routed over voids. This second component of the near-end crosstalk also depends on the number of periodic voids, and it shows saturation with large number of cutouts.

Far-end crosstalk due to vertical coupling through plane voids is also non zero, even if the cross sections above and below the perforated plane form homogenous striplines.

## References

- [1] G. Blando, J. Miller, I. Novak, J. DeLap, and C. Preston, "Attenuation in PCB Traces Due to Periodical Discontinuities", Proceedings of DesignCon 2006, Santa Clara, CA, February 6-9, 2006.
- [2] Ansoft Corporation: HFSS Version 10.1.
- [3] A. Djordjevic, R. Biljic, V. Likar-Smiljanic, T. Sarkar, "Wideband Frequency-Domain Characterization of FR-4 and Time-Domain Causality", IEEE Trans. on Electromagnetic Compatibility, Vol. 43, No. 4, November 2001.